

National Aeronautics and Space Administration
Goddard Space Flight Center
Contract No. NAS-5-3760

ST - AI - 10317

NASA TT F-9666

FACILITY FORM 602	N65-21635	
	(ACCESSION NUMBER)	(THRU)
	24	(CODE)
	(PAGES)	13
	(NASA CR OR TMX OR AD NUMBER)	(CATEGORY)

INVESTIGATION OF THE LOWER IONOSPHERE BY THE
IMPEDANCE LOW FREQUENCY RADIOSONDE METHOD

by

P. E. Krasnushkin
N. L. Kolesnikov

[USSR]

GPO PRICE \$ _____

OTS PRICE(S) \$ _____

Hard copy (HC) \$1.00

Microfiche (MF) .50

16 APRIL 1965

INVESTIGATION OF THE LOWER IONOSPHERE BY THE
IMPEDANCE LOW-FREQUENCY RADIOSONDE METHOD

Geomagnetizm i Aeronomiya,
Tom 5, No.1, pp. 55-69,
Izdatel'stvo "NAUKA", 1965

by P. E. Krasnushkin,
N. L. Kolesnikov.

SUMMARY

21635
A method of measurement of lower ionosphere parameters was worked out, consisting in the registration of input impedance of a miniature airborne antenna, sensitive to variations of electrical properties of the medium surrounding the antenna. This method was applied to measurement of electron concentration and the transport frequency of electron collisions with neutral molecules in the 50-90 km altitude range, using the 50 kc/sec frequency. The results agree well with those obtained by the methods of long and ultralong waves, of differential absorption, and also by that involving the use of high-frequency and Langmuir probes. The atmospheric pressure is measured in the 70-90 km altitude range by the transport collision frequency. It coincides with that of the standard atmosphere with a precision to 3-5 percent.

* * *

Author

Interest to lower layers of the ionosphere induced us to work out a low-frequency sonde, constituting a "nonemitting" airborne antenna, whose input impedance is sensitive to electrical properties of the medium surrounding it. At first it was applied to measurement of electron concentration, then also to that of electron collision frequency [1].

* ISSLEDOVANIYE NIZHNEY IONOSFERY METODOM IMPEDANSNOGO NIZKOCHESTOTONOGO RADIOZONDA.

Lately, a large number of various probes were installed aboard rockets with the lower ionosphere as the target for investigations [2 - 4]. That is why we feel that publication of the low-frequency probe method is quite timely.

The method under consideration, just as the other indirect methods, requires the installation of an adequate functional connection between the readings of measuring devices and the investigated ionosphere parameters. This connection is derived from the theory of microprocesses, evolving in the ionosphere plasma near the probe. The general theory of such processes, induced by variable voltage applied to the fast moving sonde, is quite complex and not yet expounded. That is why the contemporary sonde method must satisfy the following requirements: 1) the mechanism of events in the plasma, on the basis of which the measuring device operates, must have a simple theory, so that an adequately true theoretical connection can be constructed. To that effect, means have been foreseen in the experimental installation, whereby the processes complicating the sonde theory can be neutralized; 2) the chosen functional connection must be sufficiently sensitive to measured parameters of the ionosphere and must not contain fast-varying and uneasily-controllable parameters.

The method of long and ultralong waves played an important part in the development of the sonde method [5 - 8]; the detection of the C-layer of the ionosphere could be made with its help. By the time of first summer experiments with the sonde, that took place on 24 June 1954, reliable data on electron concentration N_e of the ionosphere were available to us.

#1. - LOW-FREQUENCY IMPEDANCE RADIOSONDE METHOD

1. - A miniature, collapsible-whip or T-type antenna, installed aboard the lateral surface of the rocket and fed by sinusoidal voltage with frequency $f = 50 \text{ kc/sec}$, constitutes the measuring device's pickup. The length of the vertical part of the antenna did not exceed 30 - 50 cm, and that of the horizontal parts of T-antennas - 50 to 60 cm. The antennas are made of copper tubes with 1.5 cm cross section diameter.

In the input impedance, Z , of such an antenna, equal to $R + iX$, depends on its geometrical shape, the frequency $\omega = 2\pi f$ and on the electrical properties of the surrounding medium within the limits of a region whose linear dimensions are of the order of those of the antenna (l). We shall designate this region, where R and X are sensitive to variations of medium's properties, as the zone of the sonde. The measurement method amounts to: 1) measurement of Z and 2) determination of the numerical values of the parameters of the medium from the functional link between Z and the latter.

The lower part of the ionosphere is a feebly-ionized plasma, consisting of neutral molecules, electrons, and also of positive and negative heavy ions. They are characterized by numerous parameters: 1) concentrations of n_m , N_e , N^+ and N^- ; 2) mean collision frequencies, from which we shall separate the collision frequency of electrons with neutral molecules $\bar{\nu}_{en} = \bar{\nu}$ and ions $\bar{\nu}_{ei}$; 3) Langmuir frequency of plasma oscillations ω_0 , $\omega_0^2 = 4\pi e^2 N_e / m$ where e and m are the charge and the mass of the electron; 4) gyromagnetic frequency for electrons $\omega_H = -eH_0 / mc$, where H_0 is the outer magnetic field, $c = 3 \cdot 10^8$ m/sec; gyromagnetic frequency Ω_H of ions; 5) temperatures of electrons T_e , of ions T_i and of neutral particles T .

Because of the great mass difference of electron and ion, the motion of electrons exerts the main effect upon the sonde impedance, and that is why we shall take interest in the parameters N_e and $\bar{\nu}$ in the first place.

One of the characteristic traits of a low-frequency sonde is the smallness of ω by comparison with $\omega_0 \sim 10^6$ and $\omega_H = 8.6 \cdot 10^6$. In the high-frequency sondes ω is greater than ω_H and ω_0 . Contrary to the latter, the Earth's magnetic field H_0 exerts a strong influence in the case under consideration. This effect is manifest beginning with $h > 75 - 80$ km, when $\bar{\nu}^2 \ll \omega_H^2$ and the plasma is strongly magnetized. For $h < 70$ km, $\bar{\nu}^2 \gg \omega_H^2$ and we may neglect the anisotropic plasma.

The introduction of the sonde into the plasma induces perturbations in it, varying the above-indicated parameters. The perturbations

are caused by the voltages applied to the sonde, by its motion in the plasma and by the very fact of its introduction into it. In its turn, the plasma distorts the field of the sonde. That is why in the general case, the functional relationships between R and X and the parameters of the plasma and of the sonde are very complex. They should be obtained from the joint solution of Boltzmann and Maxwell equations. We shall write these relationships, conditionally as follows:

$$\begin{aligned} R &= f_1(N_e, \bar{v}, \omega_H, \omega; \varepsilon_1, \varepsilon_2, \dots, \varepsilon_N), \\ X &= f_2(N_e, \bar{v}, \omega_H, \omega; \varepsilon_1, \varepsilon_2, \dots, \varepsilon_N), \end{aligned} \quad (1)$$

where N_e and \bar{v} are the unperturbed parameters of the ionosphere, which we propose to measure; ω_H, ω are given parameters; $\varepsilon_1, \varepsilon_2, \dots, \varepsilon_N$ are the remaining parameters of the plasma and of the sonde, whose accounting is undesirable if only in an explicit form.

The quantities R and X are measured by an electrical installation, delivering to telemetric system input, two voltages, U_1 and U_2 , linked with R and X in the general case by the equations

$$U_1 = \varphi_1(R, X), \quad U_2 = \varphi_2(R, X). \quad (2)$$

The relations (2) are obtained by calibration of the measuring device.

According to U_1 and U_2 , obtained through measurements, we may determine N_e and \bar{v} with the aid of (1) and (2) for given ω_H and ω (see for details #5). This is the simplest method of data agreement, when U_1 and U_2 are deemed reliable, the relations (1) and (2) adequately true, and N_e and \bar{v} are unknown.

2. - The deriving of functional relations (1) constitutes the source of main errors of the method. In order to simplify the form of the adequate link, we shall utilize such low field strengths at the sonde V , that the superheating of electronic gas be prevented and the temperature T_e be near that of the neutral gas T . To that effect the following inequality should be satisfied

$$E < \sqrt{\frac{3mkT}{e^2} \delta(\omega_1^2 + \bar{v}^2)}, \quad E \sim V_3/l \quad \omega_1 = \omega + \omega_H, \quad (3)$$

where k is the Boltzmann constant, δ is the mean relative fraction of energy lost by an electron at collision with a molecule. Under conditions of lower ionosphere, the inequality (3) is fulfilled for $|E| < 0.25$ v/m. The voltage V_E applied by us to the sonde, did not exceed 0.15 v, and (3) was not fulfilled. In this case, the plasma may be considered as a medium characterized by the tensor of the dielectric constant

$$(\epsilon) = \begin{pmatrix} \epsilon_{\parallel} & 0 & 0 \\ 0 & \epsilon_{\perp} - \epsilon_x & \\ 0 & \epsilon_x & \epsilon_{\perp} \end{pmatrix} \quad (4)$$

acting upon the components E_x, E_y, E_z , directed along E_x and across E_y and E_z of the Earth's magnetic field H_0 . By the strength of (3), the components (4) depend only on local properties of the plasma, that is mainly on N_e and \bar{v} , and do not depend on the field strength. The requirement of local dependence assumes, that plasma waves are absent, such for example as the electroacoustic ones [10].

Taking into account the condition for quasistationary state, i. e. $l \ll 2\pi c/\omega$, the sonde may be considered as a condensor, filled with an inhomogeneous-anisotropic dissipative dielectric, with the dielectric constant tensor (4). The condensor is characterized by the concentrated parameters $R(\omega)$ and $C(\omega)$.

Taking into account that the field of the sonde E , placed on the lateral surface of a vertically-flying rocket, mostly normally to H_0 , we shall simplify the problem by considering the sonde as a plane condensor of capacity C_0 , filled by a uniform medium with a complex dielectric constant $\epsilon_{\perp} = \epsilon_{\perp}' - i\epsilon_{\perp}''$. Then its complex conductance $Y = 1/Z$ will be

$$Y = Y' + iY'' \simeq i\omega\epsilon_{\perp}C_0 = i\omega(\epsilon_{\perp}' - i\epsilon_{\perp}'')C_0.$$

Since $Z = 1/Y$ is the input impedance, hence we obtain the functional relations (1)

$$R = \frac{1}{R_e Y} \simeq \frac{1}{\omega\epsilon_{\perp}''C_0} = \frac{1}{4\pi\sigma_{\perp}(N_e, \nu, H_0, \omega)C_0} \quad (1')$$

..//..

$$\delta C = \frac{I_m Y}{\omega} - C_0 = \delta \epsilon_{\perp}'(N_e, \bar{v}, H_0, \omega) C_0$$

$$\left(\delta \epsilon_{\perp}' = \epsilon_{\perp}' - 1, \quad \epsilon_{\perp}'' = \frac{4\pi\sigma_{\perp}}{\omega} \right), \quad (1'')$$

where C_0 is the sonde capacitance in vacuum.

For the construction of the dependence of ϵ_{\perp}' and σ_{\perp} on plasma parameters we may utilize the Lorentz equation, thus obtaining the well known expressions

$$\epsilon_{\perp}' = 1 - \frac{V(s^2 + 1 - u^2)}{(s^2 + 1 + u^2) - 4u^2}, \quad (5')$$

$$\sigma_{\perp} = \frac{\omega V s (s^2 + 1 + u^2)}{4\pi[(s^2 + 1 + u^2)^2 - 4u^2]}, \quad (5'')$$

$$(V = \omega_0^2/\omega^2, \quad s = v_{eff}/\omega, \quad u^2 = \omega_H^2/\omega^2,$$

where $\bar{v} = v_{eff}$ is the effective collision frequency, figuring in the Lorentz equation, in the so called "friction" term; $mv_{eff}(dr/dt)$. Our first calculations of N_e and v_{eff} were made by the formulas (1') and (1''), where ϵ_{\perp}' and σ_{\perp} were taken according to (5). In the following, we utilized instead of (5) the more precise formulas of the kinetic theory, which lead in the B. I. Davydov approximation [11] to the expressions

$$\epsilon_{\parallel} = 1 + i \frac{8V}{3\sqrt{\pi}} \int_0^{\infty} \frac{w^4 e^{-w^2} dw}{(s_{tr} - i)}, \quad (6)$$

$$\epsilon_{\perp} = 1 + i \frac{8V}{3\sqrt{\pi}} \int_0^{\infty} \frac{(s_{tr} - i) w^4 e^{-w^2} dw}{(s_{tr} - i)^2 + u^2}, \quad (7)$$

$$\epsilon_x = -i \frac{8Vu}{3\sqrt{\pi}} \int_0^{\infty} \frac{w^4 e^{-w^2} dw}{(s_{tr} - i)^2 + u^2}, \quad (8)$$

where $w = v/\bar{v}$ is the electron velocity brought up; $\bar{v} = \sqrt{2kT/m}$ is the most probable velocity; $s_{tr} = v_{tr}/\omega$, where v_{tr} is the transport frequency of collisions, linked with the transport collision cross section A by the expression $v_{tr} = n_m A v$, where n_m is the concentration of neutral particles. The collisions with ions are neglected in the expressions (6), (7), (8), which, as is shown by theoretical investigations, can be accounted for additionally in the $v, \bar{v} = v_{em} + v_{ei}$, without changing the form of the formulas (6), (7) and (8).

It follows from laboratory investigations [12, 13], that collisions of electrons with nitrogen molecules predominate in the lower layers of the ionosphere. For thermal electrons, colliding with nitrogen molecules, the transport collision frequency A is proportional to the velocity, $A = a_0 v$, where $a_0 = 3.29 \cdot 10^{-23}$, and not inversely proportional to v , as this would have been necessary for the formula (7) to coincide with (5). Thus, the notion v_{eff} , introduced in the elementary theory, does not correspond to real dissipation processes of electromagnetic energy taking place in the lower layers of the ionosphere. Introducing into (6), (7), (8), the most probable transport collision frequency and accordingly

$$\bar{s} = \bar{v}_{\text{tr}}/\omega = n_m \alpha_0 \bar{v}^2/\omega, \quad s = \bar{s} w^2, \quad (9)$$

we shall write (6), (7), (8) in the form

$$\delta e_{\parallel} = 1 - e_{\parallel} = \frac{8V}{3\sqrt{\pi}\bar{s}} \left[\frac{1}{\bar{s}} \Phi_2\left(\frac{1}{\bar{s}}\right) - i \Phi_1\left(\frac{1}{\bar{s}}\right) \right], \quad (6a)$$

$$\delta e_{\perp} = 1 - e_{\perp} = \frac{4V}{3\sqrt{\pi}\bar{s}} [\xi_+ \Phi_2(\xi_+) + \xi_- \Phi_2(\xi_-)] - i \frac{4V}{3\sqrt{\pi}\bar{s}} [\Phi_1(\xi_+) + \Phi_1(\xi_-)], \quad (7a)$$

$$e_x = -i \frac{4V}{3\sqrt{\pi}\bar{s}} [\xi_+ \Phi_2(\xi_+) - \xi_- \Phi_2(\xi_-)] - \frac{4V}{3\sqrt{\pi}\bar{s}} [\Phi_1(\xi_+) - \Phi_1(\xi_-)], \quad (8a)$$

$$\Phi_1(\xi) = \int_0^{\infty} \frac{w^6 e^{-w^2} dw}{w^4 + \xi^2}, \quad \Phi_2(\xi) = \int_0^{\infty} \frac{w^4 e^{-w^2} dw}{w^4 + \xi^2}, \quad (10)$$

where Φ_1 and Φ_2 are functions of the argument $\xi_{\pm} = (1 \pm u)/\bar{s}$.

The integrals Φ_1 and Φ_2 were integrated in the range of values ξ of interest to us. With their help we plotted the functions $F_1, F_2, F_3, F_4, F_5, F_6$, entering into e_{\parallel}, e_{\perp} and e_x in the following form:

$$\delta e_{\parallel} = \frac{8V}{3\sqrt{\pi}} F_1 - i \frac{8V}{3\sqrt{\pi}} F_2, \quad (66)$$

$$\delta e_{\perp} = -\frac{8V}{3\sqrt{\pi}} F_3 - i \frac{8V}{3\sqrt{\pi}} F_4, \quad (76)$$

$$e_x = -i \frac{8Vu}{3\sqrt{\pi}} [F_5 + 2iF_6], \quad (86)$$

where

.../...

$$\begin{aligned}
F_1 &= \frac{1}{\bar{s}^2} \Phi_2\left(\frac{1}{\bar{s}}\right), & F_2 &= \frac{1}{\bar{s}} \Phi_1\left(\frac{1}{\bar{s}}\right), & F_3 &= \frac{-1}{2\bar{s}} [\xi_+ \Phi_2(\xi_+) + \xi_- \Phi_2(\xi_-)], \\
F_4 &= \frac{1}{2\bar{s}} [\Phi_1(\xi_+) + \Phi_1(\xi_-)], & F_5 &= \frac{1}{2u\bar{s}} [\xi_+ \Phi_2(\xi_+) - \xi_- \Phi_2(\xi_-)], \\
F_6 &= \frac{-1}{4u\bar{s}} [\Phi_1(\xi_+) - \Phi_1(\xi_-)].
\end{aligned}$$

The functions F_k ($k = 3, 4, 5, 6$) from two arguments \bar{s} and u jointly with F_1 and F_2 are plotted in Fig. 1, where \bar{s} is taken as the abscissa, and u^2 is a parameter.

From (7) it follows, that the relation

$$|\delta \varepsilon_{\perp}' / \varepsilon_{\perp}''| = F_3 / F_4 = f(\bar{s}, u) \quad \left(\varepsilon_{\perp}'' = \frac{4\pi\sigma_{\perp}}{\omega} \right) \quad (11)$$

is independent from N_e . That is why it is practical to take (1) for one of the functional relations. It serves for the determination of \bar{v}_{tr} by the measured $\text{Im} \varepsilon_{\perp}$ and $R \varepsilon_{\perp}$. To that effect F_3 / F_4 , as a function of \bar{s} is plotted in Fig. 2.

Utilizing (1') and (1''), we shall obtain the equation searched for

$$f\left(\frac{\bar{v}_{tr}}{\omega}, u\right) = \omega R \delta C, \quad (12)$$

where R and δC are measured values. Note that for a small $1/\xi$ the following correlation takes place:

$$\frac{|\delta \varepsilon_{\perp}'|}{\varepsilon_{\perp}''} = \frac{F_3}{F_4} = \frac{1}{2.5s} = 0.4\omega / v_{tr} = \omega R \delta C. \quad (12a)$$

It may be obtained by way of expansion of subintegral expressions in (10) by powers $1/\xi$, and breaking these expansions at the second term of the series.

.../...

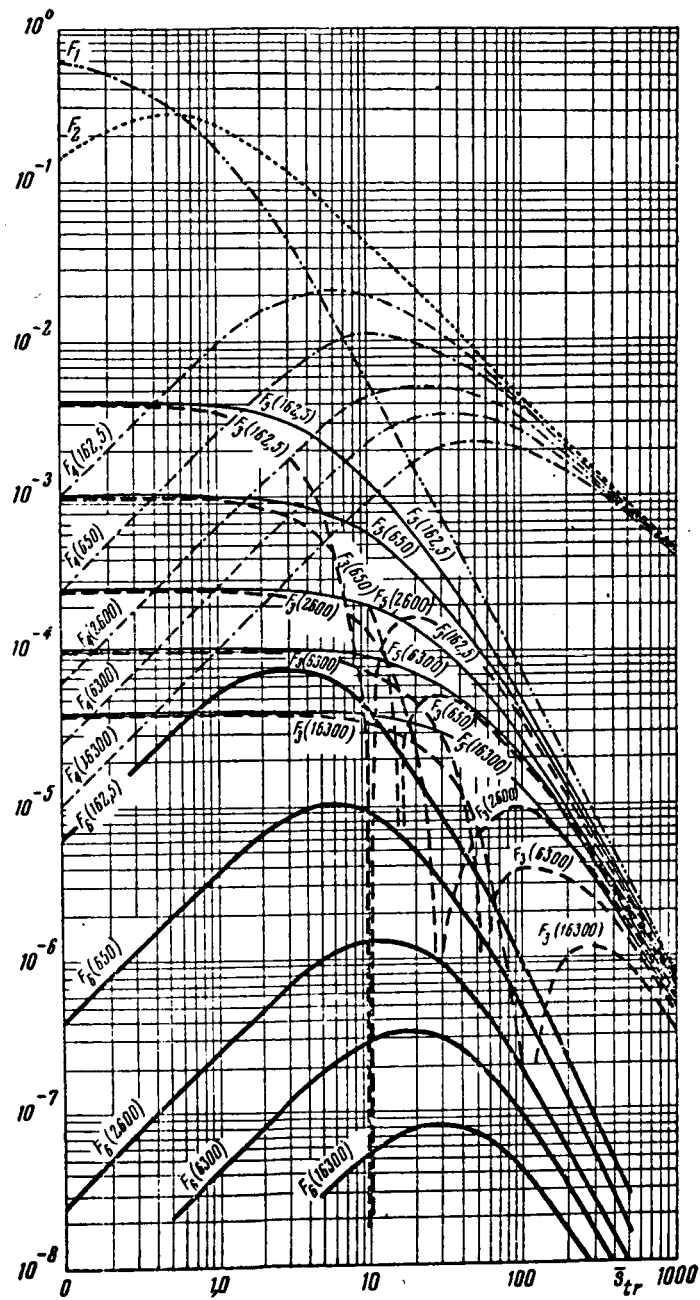


Fig. 1

Formula (12 a) is utilized for the approximate determination of \bar{v}_{tr} , when

.../...

$$\left| \frac{(1 \pm u)}{\bar{s}} \right| \gg 1, \quad \bar{v}_{tr} = \frac{0,4}{R\delta C}. \quad (126)$$

Therefore, at inequality $|1 \pm u| \gg \bar{s}$ fulfillment, the most probable transport collision frequency ν_{tr} is determined as a quantity inverse to the relaxation time of the contour with parameters R and C . In the parameter region, where $|1 \pm u| \gg \bar{s}$, $\nu_{eff} = 2,5\nu_{tr}$.

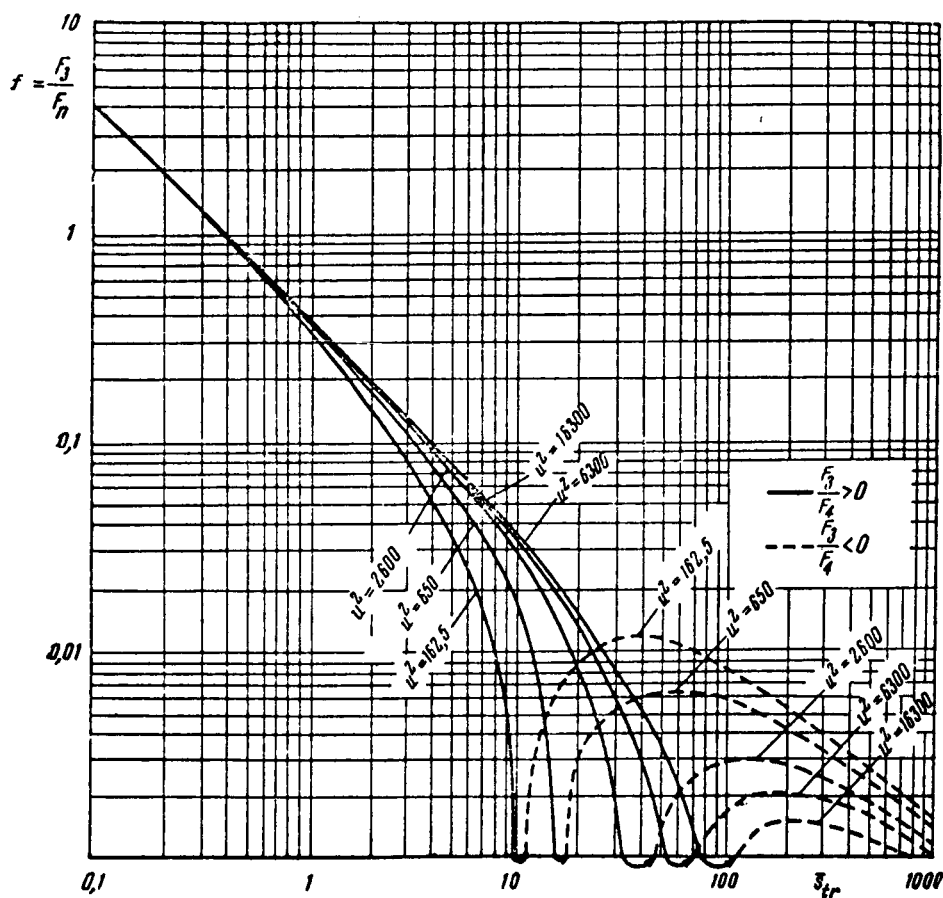


Fig. 2

After ν_{tr} has been determined, the calculation of N_e is effected with the help of any of the curves $F_3(s, u)$ or $F_4(s, u)$ by the measured R or C . The respective formulas have the form

$$N_e = \frac{\delta C_0}{C_0} \frac{3m\omega^2}{32\sqrt{\pi}e^2} \frac{1}{F_3}, \quad (13)$$

$$N_e = \frac{1}{C_0 R} \frac{3m\omega}{32\sqrt{\pi}e^2} \frac{1}{F_4}. \quad (13a)$$

3. - Measurement Errors.- In deriving (5), (12) and (13), it was assumed that the N_e and v_{eff} or \bar{v}_{tr} entering in them coincide with the respective parameters of the unperturbed plasma. One of the main measurement errors for N_e (and not for v) is linked with the perturbations of N_e , introduced by sonde and the rocket in the plasma surrounding them and with the inverse effects of the plasma upon the field of the sonde. Certain effects induce the depletion of the unperturbed ionosphere's electron concentration, others lead to its enrichment. Taking into account the possibility of compensation of the various perturbation effects of N_e , we shall review them separately.

Effect of the Wake.- As is well known, satellites, moving at great heights, leave a wake with depleted N_e and N_i . Such a wake is revealed by the strong scattering of meter radiowaves [14 - 19], and also by the oscillations of impedance of the low-frequency sonde installed on a non-stabilized satellite [20]. The theoretical calculations of satellite wakes, conducted only for a very rarefied plasma (length of the free path $\lambda \gg l$, where l is the dimension of the body) and known to us, can not be applied in our case, and we shall limit ourselves to upper estimates of the dimensions of the wake (trail). If $\lambda \gg l$, we derive from elementary thinking that the length of the trail behind the sonde is $L \sim d(v_0/\bar{v}_i)$, where v_0 is the rocket velocity, \bar{v}_i is the mean thermal velocity of ions, d is the diameter of the sonde. Because of the Earth's magnetic field L increases somewhat. In our case, $d=1.5$, $(v_0/\bar{v}_i)_{max} \sim 3$, that is $L \sim 5$ cm for an initial width of the trail of 1.5 cm and the volume, impoverished electrons, is small by comparison with the total volume of the sonde's zone. This estimate is evidently overrated for $h < 70$ km, where $\lambda < d$ and the mechanism of trail formation is entirely different. If the calculation is conducted by the standard method of supersonic aerodynamics and is reduced to bottom vacuum effect, the region of which being of lesser extent than $L \sim d(v_0/\bar{v}_i)$.

Note, that owing to rocket stabilization, the sonde in our case never hits the region of rocket's own wake.

The Debye (Langmuir) layer around the sonde isolates the constant electric field of the sonde from the remaining part of the plasma. This phenomenon can induce a decrease of N_e in this layer provided the probe's constant potential is negative, and its increase if the latter is positive.

The potential of the sonde, just as that of the whole rocket, lends itself uneasily to theoretical or experimental estimate. That is why it is impossible to account for N_e variation in this method, that is in formula (1). Fortunately, the influence of the Debye layer is insignificant.

The Debye layer has at $\bar{v}_e \gg v_0 > \bar{v}_i$ an entirely different mechanism, distinct from the effect of the wake, and its shape is little dependent on rocket velocity v_0 contrary to that of the trail [18, 19]. For this reason, the estimate of Debye layer dimensions can be made in the assumption that $v_0 = 0$. In this case the thickness of the layer is comparable with the Debye radius $D = 5\sqrt{T_e/T_n}$ and at heights $h < 70$ km, where N_e constitutes $10 - 100$ electron/cm³, it takes, at first sight, menacing dimensions: $D \sim 10$ cm. However, at these heights, the time between collisions of electrons with molecules $\tau_{em} = 1/v_{eff} \simeq 10^{-7} \div 10^{-8}$ sec is much less than the time τ_0 of incident plasma passing through the Debye layers $\tau_0 = D/v_0 \simeq 10^{-4}$, whereas τ_0 is comparable or lesser than the time of Debye layer settling $\tau_n = 1/\sigma \sim 10^{-3} \div 10^{-4}$, where σ is the conductance of the medium. That is why the Debye layer is continually blown off by the incident flow and there occurs no N_e perturbation. It can be manifest only at heights $h > 85 - 90$ km, but, because of high electron concentration in that range D does not exceed 1 cm, in other words, the possible perturbation zone is small by comparison with the total operating zone of the sonde. The absence of Debye shielding effects during the study of the lower ionosphere is not in contradiction with the investigations by Pfister [2], who, varying the constant potential V_{30} on the probe, did not notice any N_e variations during measurements by impedance sonde. Our investigations were limited to sonde length variations. They also are evidence of absence of this effect.

Effects linked with the Sonde's High-frequency Field.— The interaction of the plasma with the field in this case takes place in the same fashion it does in the case of a constant field, and it leads to sonde field and charge around it distortion. As far as we know, these phenomena were investigated only for a fixed source in the plasma, without taking into account the magnetic field. As follows from the works by Landau [30] and also [31], a transitional layer forms around the antenna, in which the field amplitude in the immediate vicinity of antenna metal, $E_1 = E_0$, where the polarization effects of the plasma are not yet manifest, passes inside the plasma to an amplitude $E_2 = E_0 / |\epsilon|$. The width of this layer in frequencies $\omega \ll \omega_0$ is comparable with the Debye screening radius D . In our case of feebly-ionized plasma, when $|\epsilon|$ is not much different from 1, the distortion of the sonde field at the expense of the transitional layer is insignificant in spite of comparatively large dimensions of the later. It is also possible that the transition layer is weakened owing to sonde motion in the plasma as a result of sweeping off the polarization charges by the incident flow. At $\omega \rightarrow 0$, when $|\epsilon| \rightarrow \infty$ and $E_2 \rightarrow 0$, the transitional layer transforms into the Debye screening layer considered above. At the field E_2 approaches the infinity (plasma resonance) if N_e is fixed. However, the field E_2 accretion is hindered by the ponderomotive forces $\sim \text{grad } |E_2|$, extruding plasma charges from the region of great E [21]. As a result, N_e drops in the operational zone of the sonde and the frequency ω_0 egresses from resonance. This effect is apparently observed in Japanese experiments with resonance probes [2]. It may also take place outside the resonance region at great V_E . Jackson and Kane detected it, while operating with a high-frequency impedance sonde at $V_E = 200$ v. The values of N_e , measured by them, resulted three times lower than the real ones, on account of ponderomotive extrusion of charges [9, 21]. Because of small $V_E \sim 0.1$ v, this effect is absent in our case.

The photoemission, caused by solar rays, can induce an increase of N_e , as was shown by experiments in USA and Japan [2]. The emerging currents on the sonde, caused by photoemission, constituted 10^{-9} a/cm² for copper electrodes. We convinced ourselves of the smallness of this effect by installing two sondes on a single rocket at diametrically opposite sides of its

frame. The same values of N_e were given by the two sondes, with a precision of 5 percent.

Rocket Degassing Effect. - As is well known, the rocket carries along a sort of a "sheath" of gas remains, ejected from the nozzle and other auxiliary devices. Particularly harmful are the small concentrations of easily ionizable atoms (Na, K), which may increase N_e , and the electro-negative gases, oxygen for example, lowering N_e . We were concerned with the last case in practice.

Thermal Ionization. - This occurs in densification jumps, and the thermal ionization is also observed when satellite reenter the denser layers of the atmosphere ($h < 100$ km); according to our calculations, this does not induce N_e variations at velocities $v_0 < 2$ km/sec.

Therefore, we may reach the conclusion on the admissibility of applying the method utilizing formulas (5), (12) and (13) for the determination of N_e , although we should be beware of the effects described in the preceding alineas.

Accounting of the Ion Component. - It is evident, that the above-considered effects of depletion and enrichment of the sonde zone by electrons, do not affect directly the precision of measurement of collision frequencies ν_{eff} and ν_{br} .

One of the main sources of measurement errors $\bar{\nu}$ is the neglecting of ions during the calculation of $\delta\epsilon_{\perp}'$ by the formulas (5) or (12). If we take these ions into account, formula (5) for the computation of ν_{eff} will take the form

$$\frac{\delta\epsilon_{\perp}'}{\sigma_{\perp}} = -\frac{4\pi(s^2 + 1 - u^2)}{\omega s(s^2 + 1 + u^2)} + \frac{mN_i}{MN_e} \frac{(s_i^2 + 1 - u_i^2)[(s^2 + 1 + u^2)^2 - 4u^2]}{\omega s(s^2 + 1 + u^2)[s_i^2 + 1 + u_i^2]^2 - 4u_i^2} \quad (14)$$

Assuming $M/m \sim 10^5$, we obtain that for $h < 70$ km, when $\nu_{eff} \sim$ and $\nu_i \sim 10^5$, N_i/N_e must not exceed $10 + 50$ if we wish to neglect the second term of (14). Since according to theoretical estimates of N_i/N_e in daytime at heights $h < 70$ km is $\sim 100 - 300$, the computation of ν_{eff} by the formulas (5) and (12) is in this case inadmissible. Then the measure-

ments of U_1 and U_2 might give an estimate of N_i / N_e , as is shown at point 5 of this paragraph (Fig. 4e), provided v_{eff} (or \bar{v}_r) are considered as known, for example, from measurements of pressure P (see formula (15)).

It should be noted also that the sensitivity of ϵ_1'' , that is of δ to N_i by comparison with ϵ_1' , is sensibly weaker, which allows the conducting of calculations by the measured U_1 with the aid of formulas (5'') or (13') provided we consider v_{eff} (or \bar{v}_r) as known (see Fig. 4d). The precision of measurement of N_e is thus found to be sufficient even at $N_i / N_e \sim 10^3$.

We have availed ourselves of this fact during two launchings (#3), where only U_1 was measured.

It is evident that the cardinal solution of the question of accounting the ions consists in the simultaneous measurement of Z in two frequencies ω_1 and ω_2 (see #5), which will allow the determination of N_e , N_i , v_{em} and v_{et} .

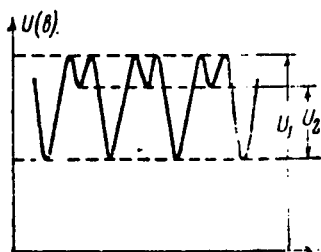


Fig. 3

4. - Measurement of sonde Z impedance is conducted by a special airborne electrical device. The principle of its operation consists in the following. The voltage of the modulation frequency Ω , produced by the low-frequency generator, controls the frequency $f_0 \pm \Delta f$ of the main generator, whose voltage is fed to a circuit of a high Q -factor, through a two-way clipper. The sonde is switched on parallelwise to the circuit. From this circuit, the voltage is taken through a small capacitance and fed to the amplifier, and then is detected. The input signal from detector has a shape sketched in Fig. 3. Let us consider two characteristic parameters of this signal — the level U_1 and the "detuning" U_2 . It is easy to see that the level of U_1 is function of resistance R of the condensor only, whereas the detuning of U_2 depends on R as well as on δC . The dependences $U_1 = \varphi_1(R)$ and $U_2 = \varphi_2(R, \delta C)$ will be taken as functional relations (2). They are obtained by way of calibration of the above-described scheme switching different R and δC to the sonde, and registering U_1 and U_2 . The calibration is carried out jointly with the telemetric system. By reconstructing and changing the sonde, and varying the way of switching it to circuit, the measurement scheme allows to encompass the range of measured values: $\epsilon_1' = \pm 10^2$; $\delta = 10^{-8} \div 10^2$ mo/m.

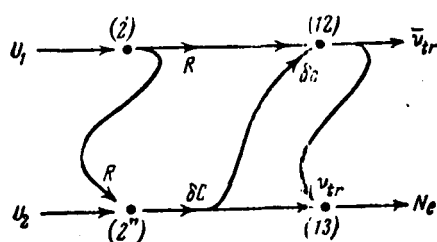


Fig. 4a

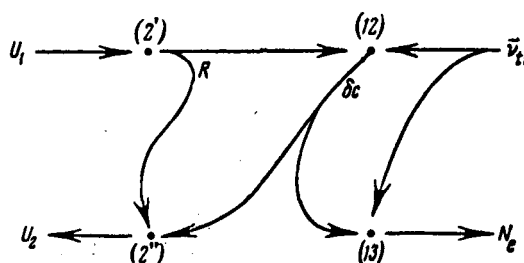


Fig. 4

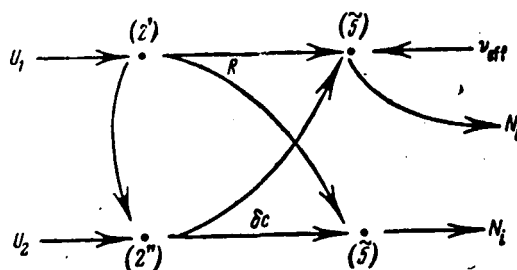


Fig. 4

5.- The entire procedure of obtaining the ionosphere parameters N_e and \bar{v}_{tr} according to the measured values of U_1 and U_2 may be represented in the form of an oriented graph (Fig. 4a). Here the links between the formulas are plotted by graph's arcs, and the transformations themselves of input to output data - by its summits. The first are marked by arrows directed toward summit, the second - by arrows, emerging from the summit. Alongside with summits indicated are the numbers of formulas, by which the transformation of input data into the output ones is made. The transformations by formulas (2) are given by graphs of Fig. 5, where the upper index $U_{1,2}^{(k)}$, $k = 1, 2, 3, \dots, 6$ indicates the number of the measurement (see #2). For the formula (12) and the second formula (13) we utilized the graphs of Figs. 1 and 2. For the determination of v_{tr} and N_e , formulas (5', 5'') are used instead of (12, 13). If only one U_1 is measured, we may, considering v_{tr} as known, find N_e with the aid of processing the data according to the graph of Fig. 4b. In the case, when the concentration of ions is strongly differing from N_e , we may determine N_e and N_i by introducing into (5) or (12, 13) the terms with N_i , according to the given \bar{v}_{eff} (or \bar{v}_{tr}) and the measured U_1 and U_2 , as is shown in the graph Fig. 4c. It is indicated by the tilde sign, that N_i is taken into account in (5) according to (14). It is evident, that all the four plasma parameters N_e , \bar{v} , N_i , v_{ei} can be determined by the measured R and δC in two frequencies ω_1 and ω_2 .

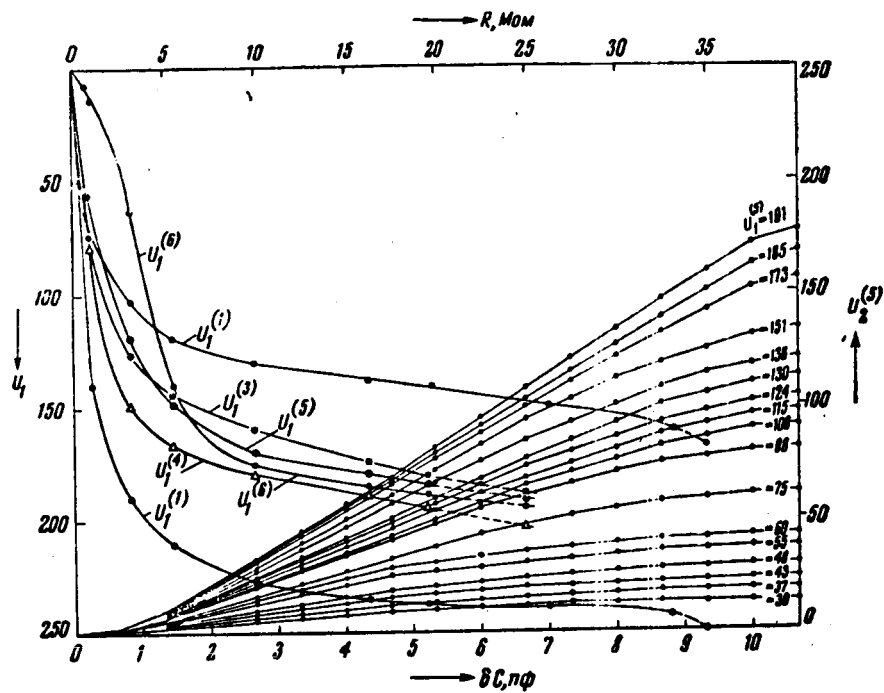


Fig. 5

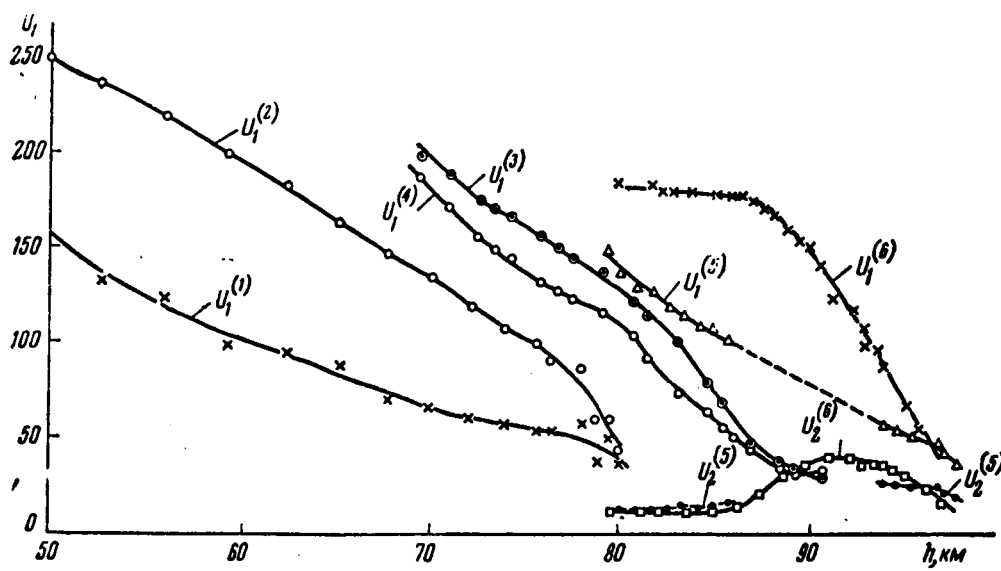


Fig. 6

#2. - RESULTS OF MEASUREMENTS OF N_e AND v_{eff} OR \bar{v}_{tr}

Assembled in Fig. 6 are the curves $U_1^{(k)}$ and $U_2^{(k)}$ obtained in three launchings: 1) at 15 30 hours LT on 24 June 1954; 2) at 09 47 hours LT on 2 August 1958; , respectively $U_1^{(1)}$, $U_1^{(2)}$ and $U_1^{(3)}$, $U_1^{(4)}$; 3) at 07 40 hours on 2 July 1959; $U_1^{(5)}$, $U_2^{(5)}$ and $U_1^{(6)}$, $U_2^{(6)}$. According to observatory and local ionospheric station data, the Sun and the ionosphere were quiet during the periods of the second and third launchings, while during the first launching a strong sporadic E_s -layer was observed. Two sondes were used at each launching; they were installed on diametrically opposed sides of the rocket, in its middle part.

We shall begin the consideration from the third, most complete measurement. The processing was conducted according to graph Fig. 4 a. The following quantities were determined for C_0 in micromicrofarads $C_0^{(5)} = 17,75$, $C_0^{(6)} = 4,95$; $C_0^{(3)} = C_0^{(4)} = 12,7$ and $C_0^{(1)} = C_0^{(2)} = 9,39$. At the outset the processing was conducted by formulas (5) in agreement with the graph of Fig. 4. The values of $N_e(h)$ and $v_{eff}(h)$ thus obtained are plotted in Fig. 7. Every curve here is the average result of two measurements obtained in a single experiment. $N_e(h)$ is significantly less than the midday $N_e(h)$ obtained by [5 - 8]. This is explained by early observation hours. At middle latitudes, where launching took place, the zenithal angle of the Sun was $\chi = 51^\circ$ and the height of the ionosphere in the D-layer was by about 10 km higher than the midday (noon) altitude.

Of particular interest is the curve $v_{eff}(h)$. It gives for v_{eff} a value approximately twice as small as than provided by the theoretical curve by Nicolet [22]. This result is founded in the assumption that for $h = 75 - 90$ km, $N_i/N_e < 10 + 50$.

Our conclusion as regards the overrated values of v_{eff} by Nicolet agrees well with the measurements conducted by Kane [23], having applied the method of differential absorption in the 65 - 85 km altitude range (see the curve o in Fig. 7). It should be noted that his measurements correspond to a period of strong disturbances in the ionosphere, when N_e was more than by one order greater than the normal, which precisely gave the possibility of conducting measurements by such little sensitive a method. One may assume, however, that the pressure and

consequently v_{eff} also, were near normal at these heights.

Subsequently, the processing of the results was effected by the formulas (12) and (13). The values of N_e thus found resulted near those obtained from formulas (5). The curve $\bar{v}_{\text{tr}}(h)$, computed by this method, is plotted in Fig. 7. It constitutes the extension of the curve $\bar{v}_{\text{tr}}(k)$ recomputed by Kane from v_{eff} after the works [12, 13] became available. The general curve for \bar{v}_{tr} , obtained by Kane and ourselves, agrees well with the curve for the pressure P according to the formula

$$\bar{v}_{\text{tr}}(h) = 1.2 \cdot 10^8 P(h) \text{ mm Hg} \quad (15)$$

derived by Huxley from laboratory observation data [12]. Hence, we may derive the conclusion, that the low-frequency sonde method appears to be a practical means for the determination of pressure P in the upper atmosphere through 90 km heights. One may assume, that it will ensure measurements of P with a precision to 10 percent, that is competing with the standard methods of pressure measurement [25, 32] (see the curve $P(h)$ in Fig. 7).

The deflection of $v_{\text{eff}}(h)$ for $h > 90$ km from the theoretical value $v_{\text{eff}} = 2.5 \bar{v}_{\text{tr}}$ can be ascribed to the neglecting of ion concentration in formulas (5) and (7), provided, of course, it is not a measurement error. Note that numerous sonde measurements register an overrated ion concentration at these heights [2], which is possibly connected with the ionic layer wrapping the probe.

The results of launchings during the years 1954 and 1958 were processed by a method, represented by the graph of Fig. 4, where \bar{v}_{tr} was considered given by the formula (15). The dependences $N_e(h)$ thus obtained, are plotted in Fig. 7. The curve for $N_e(1954)$ lies above the midday curve $N_e(h)$, obtained by the "CAB" method. The curve for $N_e(1958)$ is situated below $N_e(h)$, as this is required by the dependence of the height of the layer h_0 on the zenithal angle of the Sun: $h_0 = \log \sec \chi$.

Note that any sign of divide between the D- and E-layer is absent in both profiles of electron concentration $N_e(h)$ 1958 and $N_e(h)$ 1959, encompassing the D-layer and the lower part of the E-layer. This, incidently, was revealed earlier [5, 7, 8], and presently, it can be reliably ascertained

that no sharply outlined maximum of $N_e(h)$ exists in the D-layer. Such a viewpoint is confirmed by later sonde measurements by Sagalin and Smiddy [26], Pfister [20]. Smith [27] and others, brought out in Fig. 7 for the sake of comparison.

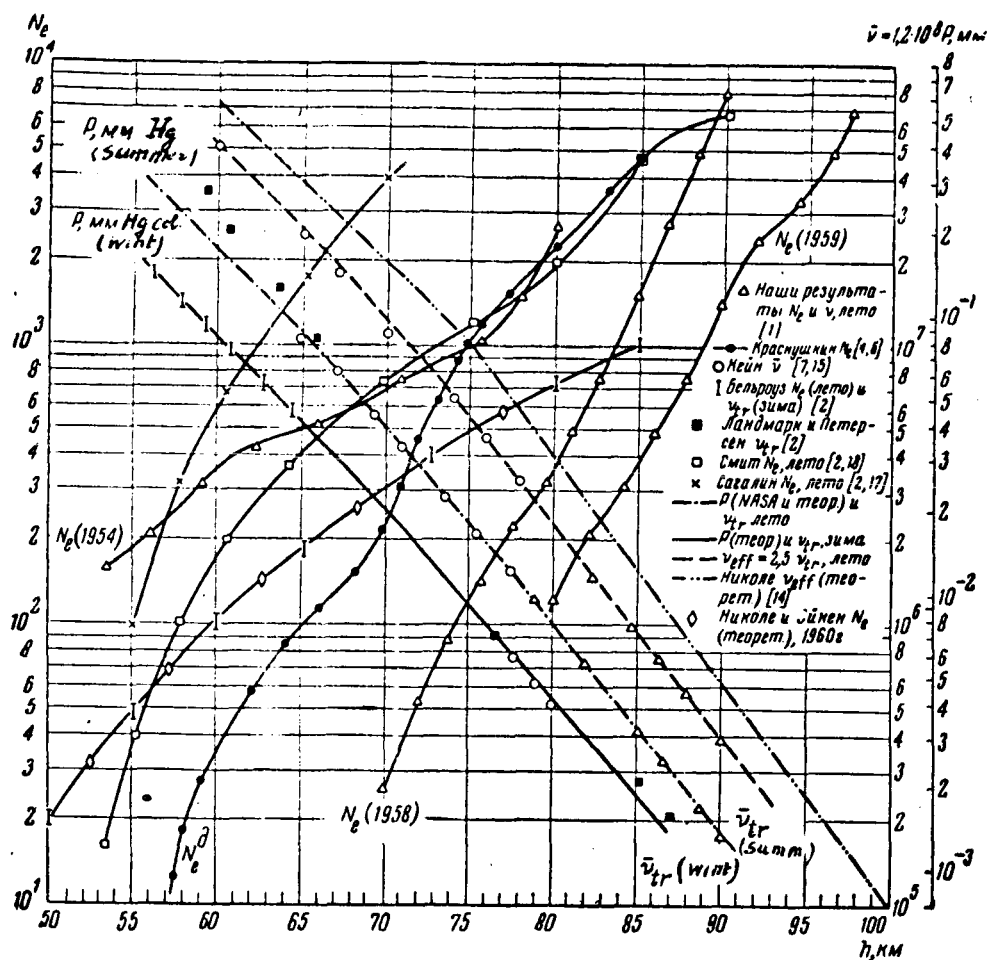


Fig. 7

Explanations

- Δ Our results for N_e and v (summer) [1]
- \bullet Krasnushkin's N_e [4, 6]
- \circ Kane's \bar{v} [7, 15]
- \square N_e (summer) and v_{tr} (winter) according to [2]
- \blacksquare v_{tr} according to Landmark & Peterson [2]
- \square Smith's N_e (summer) [2, 18]
- \times Sagalin's N_e (summer) [2, 17]
- P according to NASA and theory and v_{tr} (summer)
- P (theoretical) and v_{tr} (winter)
- $v_{eff} = 2.5 v_{tr}$ (summer)
- Nicolet's v_{eff} (theor.) [14]
- \diamond Nicolet and Aikin's N_e (theor.) [29] (1960)

Unfortunately, for most of our daylight launchings a disruption of telemetry was observed at rocket entry into the ionosphere, and that is why measurements of N_e and v_{eff} failed as a rule, below 75 km. Only the first measurement of 1954 figures amongst the small number of experiments when telemetry was operative at ionosphere entry.

CONCLUSIONS

1.- The worked out method of low-frequency impedance sonde allows the conducting of measurements of $N_e(h)$ vertical profiles in the altitude interval $50 < h < 90$ km, using one frequency, at any time of the day, and those of $v(h)$ in the interval $70 < h < 90$ km in daytime.

2.- The measured $N_e(h)$ agree with the profiles obtained in [5, -8] by the ΔB and $C\Delta B$ methods. The measured $v_{eff}(h)$ in the interval $h = 70 \div 90$ km were found to be twice as small as the theoretical values according to Nicolet [22]. This result agrees with the measurements by Kane, Jackson [9], Landmark and Peterson [28], obtained in summertime.

3.- A method of pressure measurement by \bar{v}_{tr} is proposed, which, contrary to v_{eff} , is not dependent on frequency ω and adequately explains the damping of radiowaves in the lower layers of the ionosphere. The pressure profile $P(h)$ is computed by the measured $\bar{v}_{tr}(h)$ using formula (15). It coincides for the summer with a precision to 5% with the standard atmosphere profile, which apparently refers to summertime. The winter values of v_{tr} are 30 - 50% lower than the summer values, which agrees well with the drop of P in wintertime [32].

4.- For $h < 70$ km in daytime and for $h < 80$ km in nighttime, when $\lambda = N_i/N_e > 10 \div 5$ and considering $\bar{v}_{tr}(h)$ as given by the formula (15), the method allows to measure $N_e(h)$ and $\lambda(h)$.

5.- In case of impedance Z measurement in two frequencies, it may provide simultaneously the profiles for $N_e(h)$, $N_i(h)$, $\bar{v}_{tr}(h)$ and $v_i(h)$.

6.- Graphs are given (Fig. 1) for the determination of all the tensor (ϵ) components of lower ionosphere's dielectric constant by the given ω , N_e , \bar{v}_{tr} and ω_H . At $v_{tr}/|\omega \pm \omega_H| < 0,1 \div 0,5$ the computation of (ϵ)

using the graphs of Fig.1 provides results close to those obtained by Appleton-Hartry formulas, provided one estimates in them $v_{\text{eff}} = 2.5 \bar{v}_{\text{tr}}$. Therefore, the graphs of Fig.1 should be only applied for the and methods.

The proposed method for processing the experimental results ought to be applied when the vertical component of the Earth's magnetic field prevails.

*** THE END ***

Mathematica Institute in the name
of V. A. Steklov
of the USSR Academy of Sciences.

Received on 14 Sept. 1964.

Contract No. NAS-5-3760
Consultants & Designers, Inc.
Arlington, Virginia

Translated by ANDRE L. BRICHANT
on 13-16 April 1965

REFERENCES

- [1].- P. E. Krasnushkin, N. L. Kolesnikov.- Dokl. A. N. SSSR, 146, 3, 596, 1962.
- [2].- Aeronomy Report No. 1.- Ed. by S. A. Bowhill, Univ. Ill. Urbana, 1963.
- [3].- G. S. Ivanov-Kholodnyy. Geomagnetizm i Aeronomiya, 4, 3, 417, 1964.
- [4].- R. E. Bourdeau.- Space Sci. Rev., 1, 4, 683, 719, 1963.
- [5].- P. E. Krasnushkin.- Nuovo Cimento Suppl. 26, 1, 50, 1962.
- [6].- P. E. Krasnushkin, N. A. Yablochkin.- Teoriya rasprostraneniya sverkh-dlinnykh voln (Theory of ultrahigh wave prop.) Tr. Soyuznogo NIN, 4, (12), 1955.
Reedited VTS A. N. SSSE, 1963.
- [7].- P. E. Krasnushkin.- Dokl. A. N. SSSR, 139, 1, 67, 1961.
- [8].- P. E. Krasnushkin.- Ib. 140, 4, 783, 1961.
- [9].- J. E. Jackson, J. A. Kane.- J. Geophys. Res. 64, 1074, 1959.
- [10].- H. A. Whale.- Ib. 68, 415, 1961.
- [11].- B. I. Davydov.- ZhETF., 7, 1069, 1937.
- [12].- L. G. Huxley.- J. Atm. Terr. Phys. 16, 46, 1959.

continued../..

References continued.

- [13].- A. V. Phelps, I. L. Pack.- Phys. Rev. Letters, 3 (7), 340, 1959.
 - [14].- I. D. Kraus.- Proc. I.R.E., 46, 611, 1958.
 - [15].- A. Flambard, M. Reyscat.- L'Onde électrique, No. 381, 830, 1958.
 - [16].- C. R. Roberts, Kirchner, D. W. Bray.- Proc. I.R.E., 47, 1156, 1959.
 - [17].- L. Kraus, K. Watson.- Phys. Fluids, 1, 480, 1958.
 - [18].- A. V. Gurevich.- Sb. "ISZ" (AES), Vyp. 7, 101, 1961.
 - [19].- L. P. Pitayevskiy.- Geom. i Aeronom. 1, 2, 209, 1961.
 - [20].- W. Pfister, J. C. Ulwick.- Cospar SSS III, 517, Wash. 1962
 - [21].- G. G. Getmantsev, N. G. Denisov.- Geom. i Aeronom. 2, 4, 691, 1962.
 - [22].- M. Nicolet.- J. Atm. Terr. Phys., 3, 200, 1953.
 - [23].- J. A. Kane.- J. Geophys. Res. 64 (2), 133, 1959.
 - [24].- J. A. Kane.- Ib. 23, 538, 1961.
 - [25].- E. G. Shvidkovskiy.- Tr. TsAO, vyp. 29, 1960.
 - [26].- R. C. Sagulin, M. Smiddy.- Cospar IV, Warsaw, 1963
 - [27].- L. G. Smith.- J. Geophys. Res. 67 (4), 1658, 1962.
 - [28].- B. Landmark, O. Peterson.- Aeronomy Rep. No. 1, Un. Ill. Urbana 1963
 - [29].- M. Nicolet, A. C. Aikin.- J. Geophys. Res. 65, 1469, 1960.
 - [30].- L. D. Landau.- ZhETF, 16, 574, 1946.
 - [31].- Ya. L. Al'pert, A. V. Gurevich i L. P. Pitayevskiy.- Iskusstvennyye sputniki v razrezhennoy plazme. Izd. NAUKA, 1964
 - [32].- W. Nordberg.- Aeronautics and Astronautics, 2 (5), 48, 1964.
-

ST - AI - 10 317 [80 cc]

D I S T R I B U T I O NG O D D A R D S F C

600 TOWNSEND
 STROUD
 610 MEREDITH
 SEDDON
 611 McDONALD
 ABRAHAM
 BOLDT
 612 HEPPNER
 NESS
 613 KUPPERIAN [3]
 614 LINDSAY
 WHITE
 615 BOURDEAU
 BAUER
 AIKIN
 STONE
 GOLDBERG
 JACKSON
 640 HESS [3]
 HARRIS
 MAEDA
 643 SQUIRES
 660 GI for SS [5]
 252 LIBRARY [3]
 256 FREAS
 651 SPENCER
 NEWTON
 NORDBERG

N A S A H Q S

SS NEWELL, CLARK
 SG NAUGLE
 SCHARDT
 SCHMERLING
 DUBIN
 SL LIDDEL
 GAUGLER
 FELLOWS
 HIPSHER
 HOROWITZ
 SM FOSTER
 ALLENBY
 GILL
 BADGLEY
 RR KURZWEG
 RRP GESSOW
 RRA WILSON
 RTR NEILL
 ATSS SCHWIND [5]
 WX SWEET

O T H E R C E N T E R S

A M E S R . C .
 SONETT [5]
 LIBRARY [3]
LANGLEY R.C.
 160 ADAMSON
 HESS
 213 KATZOFF
 231 O'SULLIVAN
 235 SEATON
 185 WEATHERWAX [2]
J P L
 SNYDER [3]
U C L A
 COLEMAN
U . M I C H .
 ARNOLD
M I T
 BARRETT
U C B E R K E L E Y
 WILCOX